2013-9

Experimental Microwave Breast Cancer Detection with Oil-on-Gelatin Phantom

Giuseppe Ruvio
Technological University Dublin, Giuseppe.Ruvio@dit.ie

Raffaele Solimene
Seconda Università di Napoli

Antonio Cuccaro
Seconda Università di Napoli

Jacinta Browne
Dublin Institute of Technology

Domenico Gaetano
Dublin Institute of Technology

See next page for additional authors

Recommended Citation

G. Ruvio, R. Solimene, A. Cuccaro, J. E. Browne, D. Gaetano, and M. J. Ammann. (2013). Experimental Microwave Breast Cancer Detection with Oil-in-Gelatin Phantom", *International Conference Electromagnetics in Advanced Applications*, Torino, Italy, Institute of Electronic & Electrical Engineers Antennas and Propagation Society & URSI, pp. 871-874. doi:10.1109/ICEAA.2013.6632362

Experimental Microwave Breast Cancer Detection with Oil-on-Gelatin Phantom

G. Ruvio[1, 2], R. Solimene[2], A. Cuccaro[2], J.E. Browne[3], D. Gaetano[4] and M.J. Ammann[4]

Abstract– **This paper presents a 2-D breast phantom which was realized with oil-in-gelatin materials for the evaluation of three different tumor detection methods operated in the microwave spectrum 1 – 3 GHz. A planar monopole antenna was used to scan the phantom in a multi-monostatic configuration across 36 angular locations. Results show a better performance of an Interferometric-MUSIC approach when compared to Non-coherent Migration and Wide Band MUSIC.**

1 INTRODUCTION

Limitations of conventional X-ray mammography has induced a recent interest into radio frequency based diagnostic approaches in order to take advantage of the sharpest dielectric contrast between benign and malignant breast tissues in the microwave frequency range [1]. Dielectric contrast is notably higher than the radiographic density exploited by X-ray mammography. Consequences of the superior sensitivity of RF-based techniques can have a huge social and cost impact. By reducing the false response percent, a dramatic reduction of costs for the health system together with a diminution of traumatic experiences for the patients can be achieved. The antenna properties play a fundamental role in the design of an RF breast cancer imaging system. Ultra-wideband (UWB) antennas are suitable candidates for this application as they can offer very large operating band, stable radiation properties and compact dimensions [2]. In the allocation of the operating bandwidth, the bottom edge frequency plays a very critical role. In fact, the RF signal can penetrate more efficiently when radiated at low frequencies. However, this requirement must be compromised with the overall size of the antenna. In order to improve miniaturization and impedance matching, antennas are generally immerged into a coupling medium.

Development and testing of medical imaging modalities are largely aided by using phantoms that closely mimic the physical properties of various human tissues. This task becomes very difficult when a large operating frequency range is required. In this paper a breast phantom realized from oil-in-gelatin emulsions is presented. These tissue-mimicking materials are able to reproduce the electric properties of different breast normal and malignant tissues [3]. This is achieved by varying percentages of a 50% kerosene - 50% safflower oil solution which allows materials with a wide range of dielectric properties to be constructed. An essential property of these materials is the capability to create heterogeneous and anthropomorphic structures with long-term stability of mechanical and electromagnetic properties. Due to their gelatinous consistence, these materials are significantly convenient for easy and inexpensive manufacturability. The detection of a 5-mm diameter tumor was evaluated through a printed monopole antenna that scanned the phantom in a mono-static radar configuration. Measurements are processed through three different linear non-coherent detection techniques such as migration [4], Wide Band Multiple Signal Classification, MUSIC [5] and Interferometric MUSIC [6]. The resultant reconstructions are compared and evaluated in terms of Full-Width-Half-Maximum, FWHM, Signal-to-Clutter Ratio, SCR, Signal-to-Mean Ratio, SMR, and Spatial displacement, SD.

2 MEASUREMENT SETUP

Measured data were collected in the frequency domain across 36 scanning positions uniformly distributed around the phantom. The system *antenna + phantom* was immersed into a coupling medium which presents equivalent properties to the adipose tissue. This medium improves coupling from the antenna to the phantom and also enables antenna miniaturization.

2.1 The phantom

Breast phantoms based on oil-in-gelatin emulsions can reproduce the electric properties of various normal and malignant breast tissues. A breast phantom was manufactured in order to reproduce a heterogeneous 2-D phantom with stable mechanical and electromagnetic properties (Fig. 1a). This was achieved by properly mixing the 50% kerosene - 50% safflower oil solution with a formaldehyde-based emulsion. The following oil-percentage were used to make the tissues: 80%-oil concentration for the adipose tissue, 40%-oil for fibroconnective tissue, 30%-oil for fibroglandular and skin tissues, 20%-oil for the tumor. The phantom has an overall diameter of 114 mm including the 2-mm thick skin. The fibroconnective and fibroglandular regions have 68 mm and 20 mm diameters, respectively. The dispersive behavior of skin, adipose, fibro-connective, fibro-glandular and tumor properties was

[1]Trinity College Dublin, CTVR, Dunlop Oriel House, Dublin 2, Ireland, e-mail: ruviog@tcd.ie, tel.: +353 01 4024716.
[2]Seconda Università di Napoli, DIII, via Roma 56, Aversa, Italy.
[3]Dublin Institute of Technology, School of Physics, Kevin St., Dublin 8, Ireland.
[4]Dublin Institute of Technology, Antenna and High Frequency Research Centre, Kevin St., Dublin 8, Ireland.

measured over a large frequency range spanning from 500 MHz to 4 GHz using a coaxial probe [7] (Fig. 1b). In order to create a challenging detection scenario, the 5-mm diameter tumor was asymmetrically located inside the fibrograndular region.

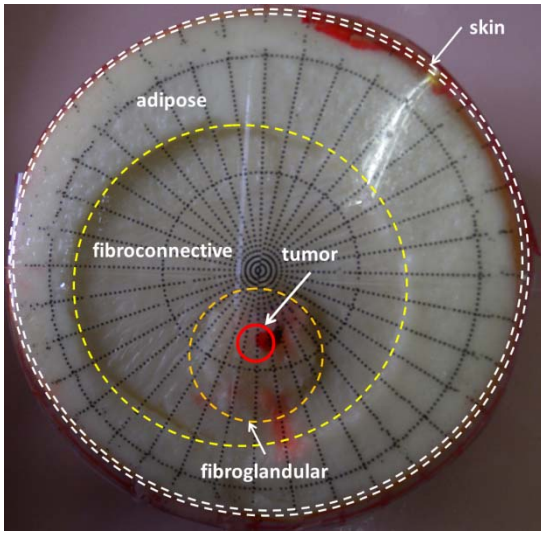

(a)

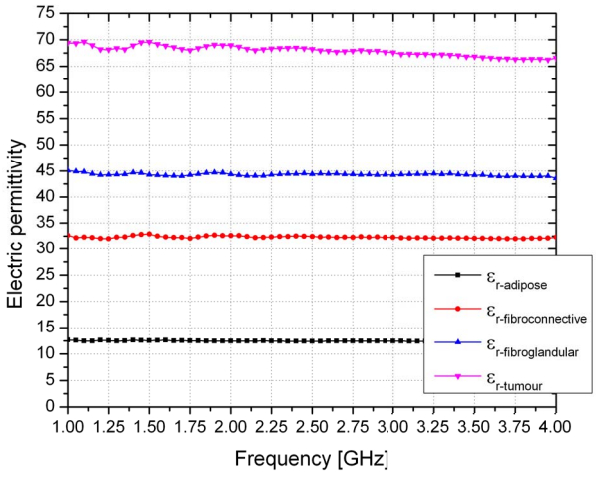

(b)

Figure 1: (a) Cross-section of the phantom; (b) Measured electric permittivity of tissues.

2.2The antenna

The planar monopole was optimized to operate across the frequency bandwidth ranging from 1 to 3 GHz when immerged into the coupling medium. In Figure 2 the geometry of the antenna is displayed. The antenna has been realized with a 1.58 mm thick Taconic CER10 substrate, which presents a stable electric permittivity of 10 across the operating frequency range. The bottom edge of the radiating element has been beveled to extend a good impedance match over a larger range of frequency.

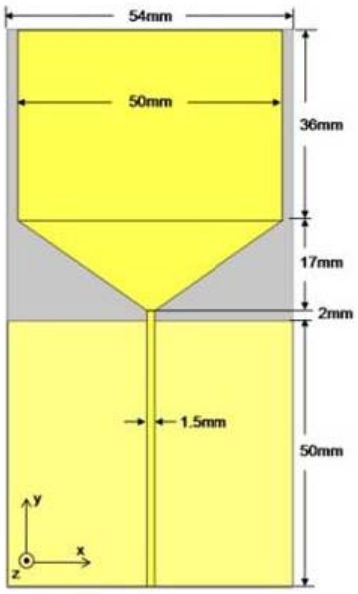

Figure 2: Antenna geometry.

3 DETECTION ALGORITHMS

Considering N TX/RX scanning positions of the antenna around the phantom ($\underline{r}_{o1}, \underline{r}_{o2}, \ldots, \underline{r}_{oN}$) and Nf the number of frequency samples, the data of a complete scan can be arranged in the $N_f \times N$ scattering matrix $\mathbf{S} = [\underline{S}^1 \ldots \underline{S}^n \ldots \underline{S}^N]$ where $\underline{S}^n$ is the column vector of data collected at the n-th position across frequency. This data consists of the informative signal scattered by the tumor but also from clutter generated from other tissues and the antenna internal reflection. The clutter tends to mask the tumor signal. In order to reduce it, a subspace based technique [8] is applied.

Accordingly, $\mathbf{S}$ is expressed through its Singular Value Decomposition (SVD) as $\mathbf{S} = \mathbf{U}\mathbf{\Lambda}\mathbf{V}^H$ where $\mathbf{U}$ and $\mathbf{V}$ are unitary matrices containing the left and right singular values, respectively, $(\cdot)^H$ represents the Hermitian operator and $\mathbf{\Lambda}$ is a diagonal matrix containing the singular values $\lambda_1, \lambda_2, \ldots, \lambda_P$, in decreasing order, with $P = min\{N_f, N_g\}$. Clutter can be then mitigated by disregarding the projection of the scattering matrix on the singular functions corresponding to the highest singular values. Determining the number of projections to discard requires *a priori* information on the clutter. However, for this application it is reasonable to associate the first singular value to clutter and discard it. Accordingly, the de-cluttered data matrix is

$$\mathbf{S}_d = \sum_{k=2}^{P} \lambda_k \mathbf{u}^k \mathbf{v}^{kH} \qquad (1)$$

Finally, the scattering data vectors can be expressed at the n-th working frequency in terms of the antenna responses in TX/RX mode, $H_T(f_n)$ and $H_R(f_n)$, the vector of the objects' scattering coefficients and the propagator $\mathbf{A}(f_n)$ which maps M scatterers located at $(\underline{r}_1,\underline{r}_2, \ldots,\underline{r}_M)$ to the scattered field:

$$\underline{S^n_d} = H_R(f_n)\boldsymbol{A}(f_n)H_T(f_n)\underline{b}(f_n) \qquad (2)$$

In particular, $\mathbf{A}(f_n)$ is expressed in terms of the relevant Green's function and its l-th column is:

$$\underline{\boldsymbol{A}}^l(\underline{r}_l; f_n) = \left[G^2(\underline{r}_{o1}, \underline{r}_l; f_n), \ldots, G^2(\underline{r}_{oN}, \underline{r}_l; f_n)\right]^T \qquad (3)$$

As no *a priori* information regarding the phantom is given, an equivalent homogeneous breast medium is considered to construct the Green's function. This is done by assigning the dielectric permittivity of the coupling medium to the equivalent breast medium in the Green's function expression.

As $H_T(f_n)$ and $H_R(f_n)$ in eq. (2) are unknown, data cannot be coherently combined while performing detection. However, data can be separately processed at each frequency and the corresponding reconstructions can be then suitably combined.

Three different operators were considered in this paper: Non-coherent Migration (N-M), Wide Band MUSIC (WB-MUSIC) and Interferometric MUSIC (I-MUSIC). Their expression is given in Table 1.

$\Phi_{N-M}(\underline{r}_k) = \sum_{i=1}^{N_f} \|M_i[\boldsymbol{A}_k(\omega_i)]\|^2$	(1)
$\Phi_{WB-MUSIC}(\underline{r}_k) = 1 \Big/ \sum_{i=1}^{N_f} \|P_i[\boldsymbol{A}_k(\omega_i)]\|^2$	(2)
$\Phi_{I-MUSIC}(\underline{r}_k) = 1 \Big/ \prod_{i=1}^{N_f} \|P_i[\boldsymbol{A}_k(\omega_i)]\|^2$	(3)

Table 1: Non-coherent operators under comparison.

where N_f is the number of adopted frequency sample and ω_i is the i-th one, $\boldsymbol{A}_k(\omega_i)$ is the steering vector calculated at the trial position $\underline{r}_k$ within the spatial domain D. Sources' positions are identified where the pseudospectrum peaks, with $P[\cdot]$ and $M[\cdot]$ being the projection operator onto the noise subspace and Migration operator [4], respectively.

4 RESULTS

The reconstructions corresponding to three different detection methods which were used to process the measurements data are shown in Fig. 3. As can be seen, those reconstructions show that under the same measurement conditions, the Intereferometric-MUSIC method presents a better performance when compared to the other non-coherent methods.

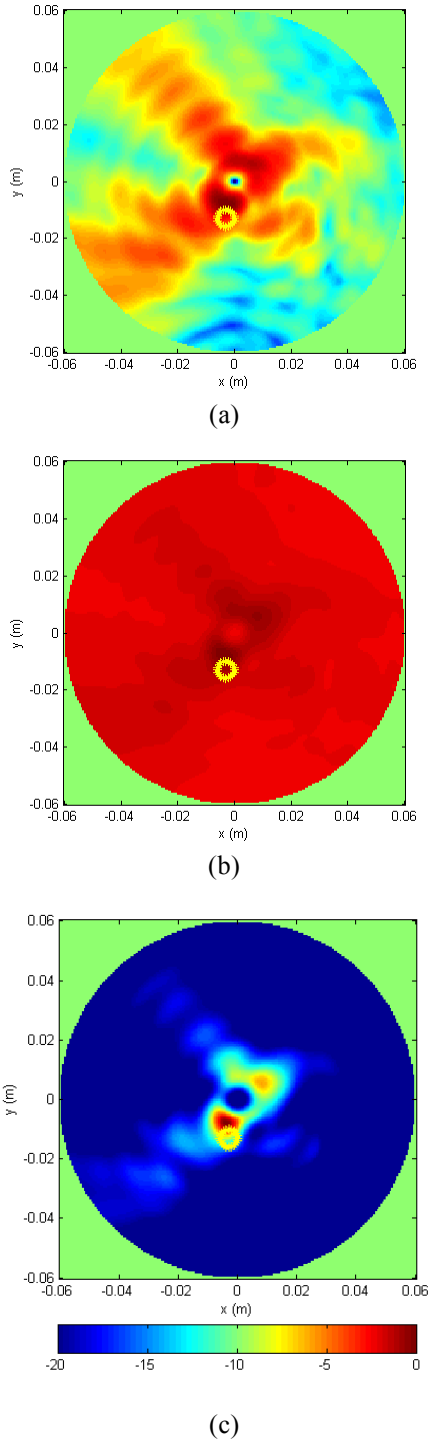

Figure 3: Reconstructions in the presence of 5-mm tumor (marked with yellow circle) by: a) Non-coherent Migration b) WB MUSIC c) Interferometric MUSIC.

The Interferometric MUSIC enables more focus and better dynamic range. Together with visual reconstructions of the detection algorithms, their performance was also measured by suitable metrics such as Signal-to-Clutter Ratio (SCR), Signal-to-Mean Ratio (SMR) and Spatial Displacement (SD) as defined in [9].The SCR and SMR compare the maximum tumor response in the reconstructed image with the maximum and the average clutter response in the same image, respectively. Whereas, The SD measures the error in tumor localization and accounts for the difference between the position of the tumor as peak value in the reconstruction and as actual center position in the scanned phantom. Results are summarized in Table 2 and confirm the superior definition achieved in reconstructions. Metrics could not be extracted for the WB-MUSIC algorithm as its dynamics is smaller than the 3-dB scale adopted for their calculation.

Method	SCR [dB]	SMR [dB]	SD [mm]
N-M	1.13	8.53	27.2
I-MUSIC	5.87	20.30	26.6

Table 2: Reconstruction metrics.

Conclusions

A 2-D oil-in-gelatin breast phantom was made for the evaluation of the scanning capability of a planar monopole antenna and three different detection algorithms. Measurements were carried out by scanning the phantom in multi-monostatic configuration across 36 uniformly distributed angles.

The Interferometric-MUSIC method offers better focusing capabilities and greater dynamic range between clutter and tumor levels when compared to standard MUSIC and non-coherent migration. Moreover, considering that the limited dielectric contrast between tumor and fibroconnective tissues and an *a priori* antenna response has not been used, the Interferometric-MUSIC system presents promising features for early stage breast cancer diagnostics.

Acknowledgments

This work was supported by Ministry of University and Research through the FIRB initiative under the project MICENEA (RBFR12A7CD), POR Campania FSE 2007/2013-"MASTRI" and the COST Action IC1102 VISTA.

References

[1] N.K. Nikolova, "Microwave Imaging for Breast Cancer," *IEEE Microwave Magazine*, Vol. 17, No. 7, pp. 78-94, 2011.

[2] G. Ruvio, R. Solimene, and M. J. Ammann, "Evaluation of Antenna Types for RF Breast Cancer Imaging using 2-Layer Planar Tissue Model", *Proc. of 40th European Microwave Conference*, Sept 2010, pp. 212–215.

[3] M. Lazebnik, E.L. Madsen, G.R. Frank, and S.C. Hagness, "Tissue-mimicking Phantom Materials for Narrowband and Ultrawideband Microwave Applications," Phys. Med. Biol. Vol. 50, pp. 4245-4258, 2005.

[4] F. Ahmad, and M.G. Amin, "Noncoherent Approach to Through-the-Wall Radar Localization," *IEEE Trans. Aerosp. Electr.Syst.*, Vol. 42, No. 4, pp. 1405-1419, 2006.

[5] M.E. Yavuz, and F.L. Teixeira, "On the Sensitivity of Time-Reversal Imaging Techniques to Model Perturbations," *IEEE Trans. Ant. Prop.*, Vol. 56, pp. 834-843, 2008.

[6] G. Ruvio, R. Solimene, A. D'Alterio, M.J. Ammann, R. Pierri, "RF Breast Cancer Detection Employing a Non-characterized Vivaldi Antenna and a MUSIC-Inspired Algorithm," *International Journal of RF and Microwave Computer-Aided Engineering*, 2013.

[7] T.P. Marsland, and S. Evans, "Dielectric Measurements with an Open-Ended Coaxial Probe," IEE Proceedings, Vol. 134, Pt. H, No. 4, pp. 341- 349, 1987.

[8] F.H.C. Tivive, M.G. Amin, and A. Bouzerdoum, "Wall Clutter Mitigation Based on Eigen-Analysis in Through-the-Wall Radar Imaging," *IEEE 17th Int. Conf. on Digital Signal Process.*, pp. 1-8, 2011.

[9] R.C. Coincecao, M. O'Halloran, M. Glavin, and E. Jones, "Comparison of Planar and Circular Antenna Configurations for Breast Configurations for Breast Cancer Detection Using Microwave Imaging," *Progress in Electromagnetics Research*, Vol. 99, pp. 1-20, 2009.